УДК 56.07 DOI:10.19110/geov.2023.7.4

Cathodoluminescence of conodont elements

A. V. Zhuravlev

Institute of Geology FRC Komi SC UB RAS, Syktyvkar; *micropalaeontology@gmail.com*

Conodont elements are used as a geochemical archive of seawater. Some compositional features of conodont elements reflect conodont ecology and trophic structure of Palaeozoic pelagic ecosystems. However, the screening of conodont elements prior to geochemical and/or isotopic studies is a real problem. This study evaluates SEM cathodoluminescence (SEM-CL), which is very sensitive to the REE and Mn content of apatite, for the detection of traces of secondary transformation in the composition of conodont bioapatite. The SEM-CL of conodont elements is similar to that of unaltered shark teeth (blue-violet), but differs significantly from that of fossil vertebrate teeth (orange-red). Thermal alteration has little effect on the SEM-CL. Elements with a CAI of 1—1.5 show a redder and more intense CL than elements with a CAI of 5. In the case of corrosion of the conodont element surface in carbonate host rocks, the CL of the outer parts of the conodont element become reddish due to invasion of the carbonate material. Conodont elements from the clay host rock show deep purple SEM-CL. Thus, SEM-CL allows detection of the results of secondary processes in conodont mineralised tissues, including enrichment by REE and/or Mn, corrosion and contamination by carbonate material. This method can be used to screen significantly altered samples prior to chemical and isotopic analyses.

Keywords: *conodonts, cathodoluminescence, mineralised tissues, taphonomy.*

Катодолюминесценция конодонтовых элементов

А. В. Журавлев

Институт геологии ФИЦ Коми НЦ УрО РАН, Сыктывкар

Конодонтовые элементы широко используются в качестве геохимического архива морской воды. Некоторые композиционные особенности конодонтовых элементов отражают экологию конодонтов и трофическую структуру палеозойских пелагических экосистем. Однако скрининг конодонтовых элементов перед геохимическими и/или изотопными исследованиями представляет собой реальную проблему. В данном исследовании оценивается катодолюминесценция (SEM-CL), очень чувствительная к содержанию REE и Mn в апатите, для обнаружения следов вторичного преобразования в составе конодонтового биоапатита. SEM-CL конодонтовых элементов сходна с таковой неизмененных зубов акул (сине-фиолетовый цвет), но значительно отличается от таковой ископаемых зубов позвоночных (оранжево-красный цвет). Термическое изменение влияет на SEM-CL конодонтовых элементов в незначительной степени. Конодонтовые элементы с ИОК = 1—1.5 демонстрируют более красноватую и более интенсивную катодолюминесценцию по сравнению с элементами с ИОК = 5. В случае коррозии поверхности конодонтовых элементов в карбонатных вмещающих породах SEM-CL внешней части конодонтовых элементов становится красноватой из-за включений карбонатного материала. Конодонтовые элементы из глинистой вмещающей породы демонстрируют темно-фиолетовый цвет SEM-CL. Таким образом, SEM-CL позволяет выявить результаты вторичных процессов в минерализованных тканях конодонтов, включая обогащение REE и/или Mn, коррозию и загрязнение карбонатным материалом. Этот метод может быть использован для выявления значительно измененных образцов перед проведением химического и изотопного анализов.

Ключевые слова: *конодонты, катодолюминесценция, минерализованные ткани, тафономия.*

Introduction

The study of the structure and composition of conodont bioapatite has yielded useful results. Conodont elements are used as a geochemical archive of seawater O and Sr isotopic composition (e.g. Luz et al., 1984; Joachimski, Buggisch, 2002; Kürschner et al., 1992; Trotter et al., 1999; Griffin et al., 2021). The carbon isotope composition of conodont elements promises to be a useful tool for reconstructing conodont ecology and trophic structure of Palaeozoic pelagic ecosystems (Zhuravlev, 2020, 2023). The Ca/Sr ratio and Ca isotope composition in conodont apatite likely reflect the position of the conodont in the food web (Balter et al., 2019; Zhuravlev et al., 2020).

The results of conodont elemental chemistry studies face the problem of distinguishing between primary and secondary geochemical signals. Usually, the thermal alteration revealed by CAI and the conodont elemental surface evaluated by SEM are the only features used to evaluate secondary changes of conodont element matter. SEM-EDS has low sensitivity for the precise study of likely geochemical exchanges between conodont elements and surrounding matter (ambient water, pore water and host rock). Therefore, screening of conodont elements prior to geochemical and/or isotopic studies is a practical issue (e.g., Zhuravlev & Shevchuk, 2017; Zhuravlev, 2023).

Cathodoluminescence (CL) is widely used to study minerals and single crystals (e.g. Richter et al., 2003; Götze, 2012). In particular, CL is used to study the composition of apatite. This method is very sensitive to the REE and Mn content of the apatite (Richter et al., 2003). Elevated Mn and REE concentrations induce orange to violet cathodoluminescence (CL) of this mineral (Ségalen et al., 2008; Wierzbowski, 2021). Cathodoluminescence analysis is used to assess the state of preservation of vertebrate teeth and conodont elements (Wierzbowski et al., 2021; Wierzbowski, 2021). The influence of diagenetic alteration on the chemical composition of bioapatites is well known (Wierzbowski, 2021). Therefore, CL appears to be useful for detecting traces of geochemical exchange between conodont bioapatite and surrounding media. Thus, CL can

For citation: Zhuravlev A. V. Cathodoluminescence of conodont elements. Vestnik of Geosciences, 2023, 7(343), pp. 36—42, doi: 10.19110/geov.2023.7.4

Для цитирования: Журавлев А. В. Катодолюминесценция конодонтовых элементов // Вестник геонаук. 2023. 7(343). С. 36—42. DOI: 10.19110/geov.2023.7.4

be used to assess secondary changes in the composition of bioapatite. In addition, the sensitivity of CL to differences in organic content and crystalline structure of apatite makes it possible to use CL as a tool for the detection of conodont element tissues.

The aim of this work is to evaluate CL as a tool for the study of conodont element histology and to assess the preservation of conodont element matter and the likely uptake of elements from host rocks.

Material

The study material comes from the Tournaisian (Lower Mississippian) shallow-water carbonate platform successions (sections in the Kamenka River basin, east of the Pechora Plate, northern Cis-Urals) and the deep-water succession (section in the Konstantinov Creek section, Cis-Polar Urals) (fig. 1).

16 polished sections of conodont elements of different morphology and preservation were examined by SEM, SEM-CL and light microscopy. Seven conodont elements from the Kamenka River sections have a CAI of 1, and nine conodont elements from the Konstantinov Creek section have a CAI of 5 (P1 elements of *Siphonodella quadruplicata* (Branson et Mehl) and *Hindeodus crassidentatus* (Branson et Mehl), and S element of *Idioprioniodus* sp.) (fig. 2). Among the conodont elements with CAI = 1, two elements (S and M) are from a clay host rock (figs. 2.9 and 2.10) and five elements (P1 of *Polygnathus parapetus* Druce) are from the limestone host rock (figs. 2.12—2.15). In addition, five conodont elements (*Pelekysgnathus isodentatus* Aristov, *Bispathodus stabilis* (Branson et Mehl) Morphotype 1, *Polygnathus communis communis* Branson et Mehl, and *Pseudopolygnathus graulichi* Bouckaert et Groessens) of different surface quality, including calcite inclusions, were examined (fig. 3).

Methods

Processing of limestone samples followed the standard procedure documented by Harris and Sweet (1989) (dissolution of limestone in 10% buffered acetic acid). Clay samples were dispersed in hot water. The residue was washed through a 70 μm sieve, dried and the conodont elements were collected.

The specimens were mounted in low molecular weight epoxy resin based on Bis A (CHS-EPOXY 520), ground and polished. The specimens were ground using UltraPrep (Buehler) diamond grinding discs before polishing with MasterPrep Sol-Gel alumina suspension. The polished surface was ultrasonically cleaned for 30 min. The polished slab was coated with C for sample conductivity in the SEM.

Light microscopy combined with SEM was used to examine the surface of the conodont elements for corrosion and the polished sections for hard tissue distribution and texture.

EDS and SEM analyses of polished sections provide data on the texture and composition of conodont hard tissues. These analyses were carried out using an Axia ChemiSEM (Thermo Scientific). EDS analysis was performed on the same SEM equipped with a TrueSight X EDS detector.

SEM-CL analyses were performed using an Axia ChemiSEM (Thermo Scientific) at an accelerating voltage of 20 kV, a working distance of 10 mm, a beam current of

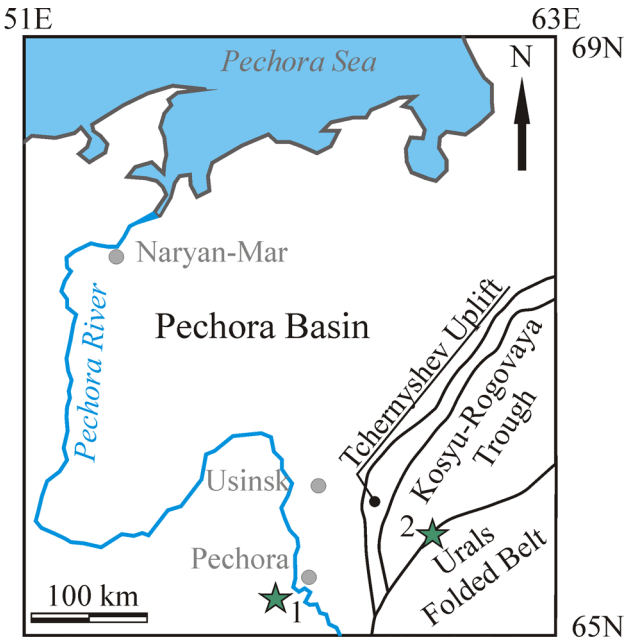

Fig. 1. Locality map: 1 — Kamenka River sections, Pechora Basin; 2 — Konstantinov Creek section, Cis-Polar Urals

Рис. 1. Схема расположения разрезов: 1 — разрез на р. Каменка, Печорский бассейн; 2 — разрез на руч. Константинов, Приполярный Урал

1.2×10^{-9} A and a dwell time of 3×10^{-5} s. The colour of the CL was evaluated on a triple plot in RGB coordinates, providing a semi-quantitative analysis of the CL. Increasing the acceleration voltage from 20 kV to 30 kV resulted in a certain red shift (in RGB coordinates) of the CL of conodont elements. Therefore, the RGB coordinates of the CL of the specimens were analysed only for the accelerating voltage of 20 kV. CL images obtained at 30 kV accelerating voltage were used for illustrations only.

Sample preparation, CL, EDS and SEM analyses were performed at Center for Collective Use of Scientific Equipment "Geonauka" of N.P. Yushkin Institute of Geology FC Komi SC UrB RAS (Syktyvkar, Russia). Original software was developed for the preparation of the triple diagram in RGB coordinates. Image analysis was performed using ImageJ software (Schneider et al., 2012).

Results

Optic microscopy and SEM

Under light microscopy and SEM, the studied conodont elements show good preservation and no traces of re-crystallisation, with the exception of one specimen (*Polygnathus parapetus* Druce from sample 122-3/16). This specimen has a corroded surface (fig. 2.15). Some conodont elements show surface contamination by carbonate particles, visible in SEM images (fig. 3).

EDS results

EDS data suggest the presence of small amounts of REE (Nd, Yb) in the conodont apatite of some samples. REE (up to 0.2 % at.) were only detected in conodont elements that came from the clayey deposit. The Mn content in the conodont apatite is below the detection threshold of the EDS instrument (< 0.1% at.). It is noteworthy that

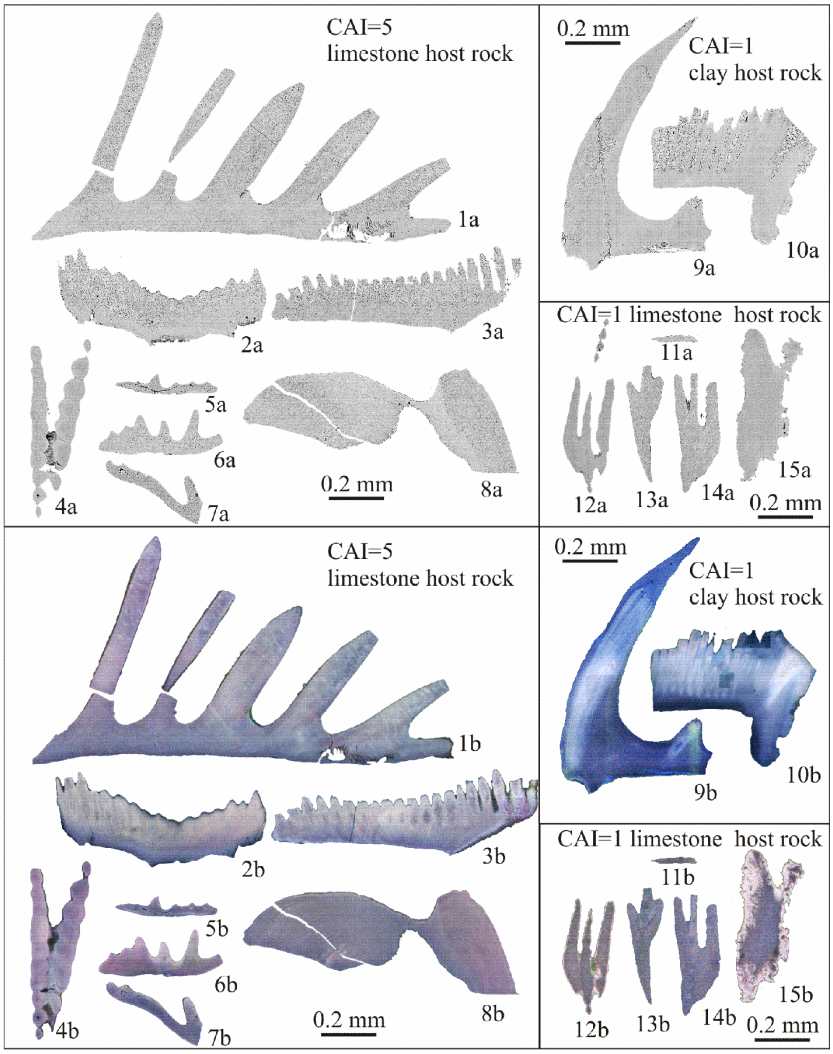

Fig. 2. SEM (a) and SEM-CL (b) images of polished sections of conodont elements. 1 — *Idioprioniodus* sp., S element, longitudinal section, sample 0-7K, the Konstantinov Creek section, middle Tournaisian; 2, 3 — *Hindeodus crassidentatus* (Branson et Mehl), P1 elements, longitudinal sections, sample 0-7K, the Konstantinov Creek section, middle Tournaisian; 4 — *Siphonodella quadruplicata* (Branson et Mehl), P1 element, oblique section of rostrum, sample 0-7K, the Konstantinov Creek section, middle Tournaisian; 5, 6 — *Siphonodella quadruplicata* (Branson et Mehl), P1 elements, transverse sections of anterior platform, sample 0-7K, the Konstantinov Creek section, middle Tournaisian; 7, 8 — *Siphonodella quadruplicata* (Branson et Mehl), P1 elements, oblique sections of platform, sample 0-7K, the Konstantinov Creek section, middle Tournaisian; 9 — S element, longitudinal section, sample 121-2-1/90, the Kamenka River section, middle Tournaisian; 10 — M element, longitudinal section, sample 121-2-1/90, the Kamenka River section, middle Tournaisian; 11 — *Polygnathus parapetus* Druce, P1 element, transverse section of free blade, sample 111A-4/19, the Kamenka River section, lowermost Tournaisian; 12 — *Polygnathus parapetus* Druce, P1 element, oblique section, sample 121-1/18, the Kamenka River section, lowermost Tournaisian; 13 — *Polygnathus parapetus* Druce, P1 element, oblique section, sample 111A-5/19, the Kamenka River section, lowermost Tournaisian; 14 — *Polygnathus parapetus* Druce, P1 element, oblique section, sample 111A-3/19, the Kamenka River section, lowermost Tournaisian; 15 — *Polygnathus parapetus* Druce, P1 element, oblique section, sample 122-3/16, the Kamenka River section, middle Tournaisian; 1b—8b — CL images are obtained at 30 kV accelerating voltage; 9b—15b — CL images are obtained at 20 kV accelerating voltage

Рис. 2. SEM-(a) и SEM-CL-(b)-изображения полированных срезов конодонтовых элементов: 1 — *Idioprioniodus* sp, S-элемент, продольный разрез, образец 0-7K, разрез на руч. Константинов, средний турне; 2, 3 — *Hindeodus crassidentatus* (Branson et Mehl), P1-элементы, продольные разрезы, образец 0-7K, разрез на руч. Константинов, средний турне; 4 — *Siphonodella quadruplicata* (Branson et Mehl), P1-элемент, косой разрез ростра, образец 0-7K, разрез на руч. Константинов, средний турне; 5, 6 — *Siphonodella quadruplicata* (Branson et Mehl), P1-элементы, поперечные срезы передней платформы, образец 0-7K, разрез на руч. Константинов, средний турне; 7, 8 — *Siphonodella quadruplicata* (Branson et Mehl), P1-элементы, косые срезы платформы, образец 0-7K, разрез на руч. Константинов, средний турне; 9 — S-элемент, продольный срез, образец 121-2-1/90, разрез на р. Каменка, средний турне; 10 — M-элемент, продольный разрез, образец 121-2-1/90, разрез на р. Каменка, средний турне; 11 — *Polygnathus parapetus* Druce, P1-элемент, поперечный разрез свободного листа, образец 111A-4/19, разрез на р. Каменка, нижний турне; 12 — *Polygnathus parapetus* Druce, P1-элемент, косой разрез, образец 121-1/18, разрез на р. Каменка, нижний турне; 13 — *Polygnathus parapetus* Druce, P1-элемент, косой срез, образец 111A-5/19, разрез на р. Каменка, нижний турне; 14 — *Polygnathus parapetus* Druce, P1-элемент, косой срез, образец 111A-3/19, разрез на р. Каменка, нижний турне; 15 — *Polygnathus parapetus* Druce, P1-элемент, косой срез, образец 122-3/16, разрез на р. Каменка, средний турне; 1b—8b — CL-изображения получены при ускоряющем напряжении 30 кВ; 9b—15b — CL-изображения получены при ускоряющем напряжении 20 кВ

the distribution of Mn in the conodont element is almost uniform and independent of that of the tissues (Trotter, Eggins, 2006).

SEM-CL of different tissues

The different tissue types distinguished by SEM and light microscopy show some differentiation on CL (fig. 4). Glow-violet CL is characteristic of albid tissue. Red-violet CL is specific for paralamellar tissue. Lamellar tissue shows deep purple CL. In general, CL images show clear tissue differentiation in brightness and weak differentiation in hue (fig. 4).

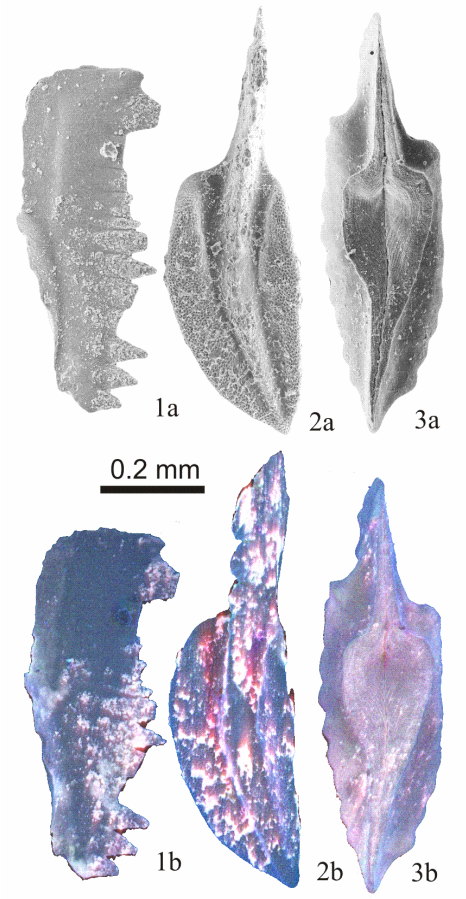

Fig. 3. SEM-(a) and SEM-CL-(b) images of conodont elements: 1 — *Bispathodus stabilis* (Branson et Mehl) Morphotype 1, P1 element, sample 101-5/19, the Kamenka River section, upper Famennian; 2 — Polygnathus communis communis Branson et Mehl, P1 element, sample 101-3/19, the Kamenka River section, upper Famennian; 3 — *Pseudopolygnathus graulichi* Bouckaert et Groessens, P1 element, sample 101-5/19, the Kamenka River section, upper Famennian. CL images obtained at 20 kV accelerating voltage

Рис. 3. SEM-(a)- и SEM-CL-(b)-изображения элементов конодонтов: 1 — *Bispathodus stabilis* (Branson et Mehl) морфотип 1, P1-элемент, образец 101-5/19, разрез на р. Каменка, верхний фамен; 2 — *Polygnathus communis communis* Branson et Mehl, P1-элемент, образец 101-3/19, разрез на р. Каменка, верхний фамен; 3 — *Pseudopolygnathus graulichi* Bouckaert et Groessens, P1-элемент, образец 101-5/19, разрез на р. Каменка, верхний фамен. CL-изображения получены при ускоряющем напряжении 20 кВ

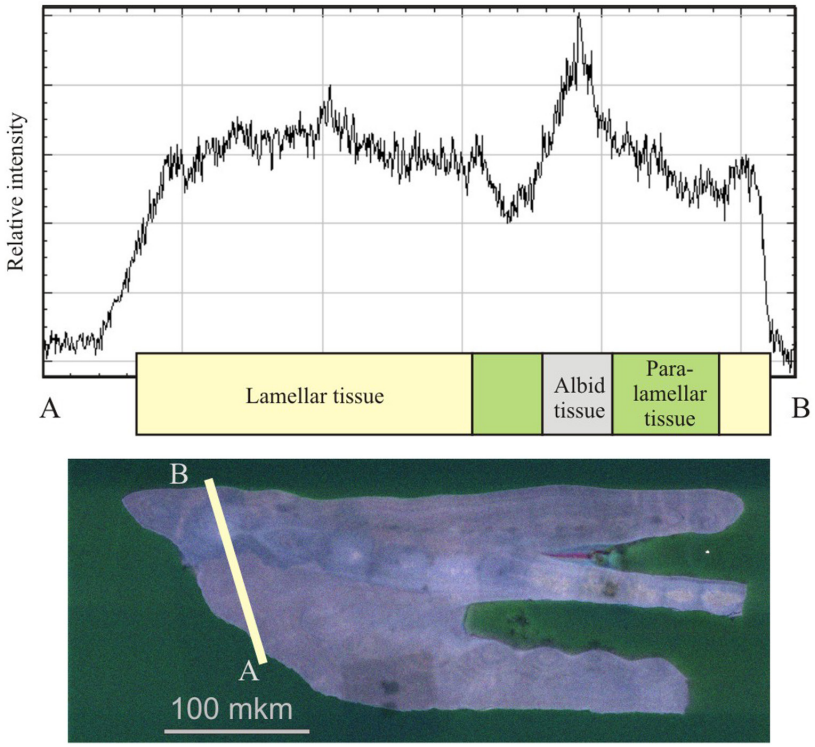

Fig. 4. Relative intensity of CL of different tissues of conodont element. Line A—B marks the position of CL intensity profile on the polished section of the P1 element of *Polygnathus parapetus* Druce (carbonate sample 111A-3/19, the Kamenka River section, lowermost Tournaisian)

Рис. 4. Относительная интенсивность CL различных тканей элемента конодонта. Линия А—В отмечает положение профиля интенсивности CL на полированном срезе P1-элемента *Polygnathus parapetus* Druce (карбонатный образец 111A-3/19, разрез на реке Каменка, нижний турне)

SEM-CL of conodont elements with different CAI and preservation

Conodont elements with different CAI show some variation in CL. Elements with a CAI of 1—1.5 show a more reddish CL compared to elements with a CAI of 5 (fig. 5, A). In general, the intensity of CL decreases in conodont elements with a CAI of 5.

Conodont elements derived from clay have more bluish CL compared to elements of the same preservation derived from limestone (fig. 5, B). Corroded conodont elements from limestone show red CL in the corroded rim (fig. 2.15, b). Unpolished conodont elements show deep blue or blue-violet CL with reddish inclusions caused by surface contamination by the carbonate material (fig. 3.2, b).

Discussion

Several factors are thought to contribute to the CL of conodont elements. Organic matter, Mn and REE appear to be the most likely inducers of conodont CL. The levels of Mn and REE may reflect either the primary composition of conodont elements or secondary element uptake from the host rock.

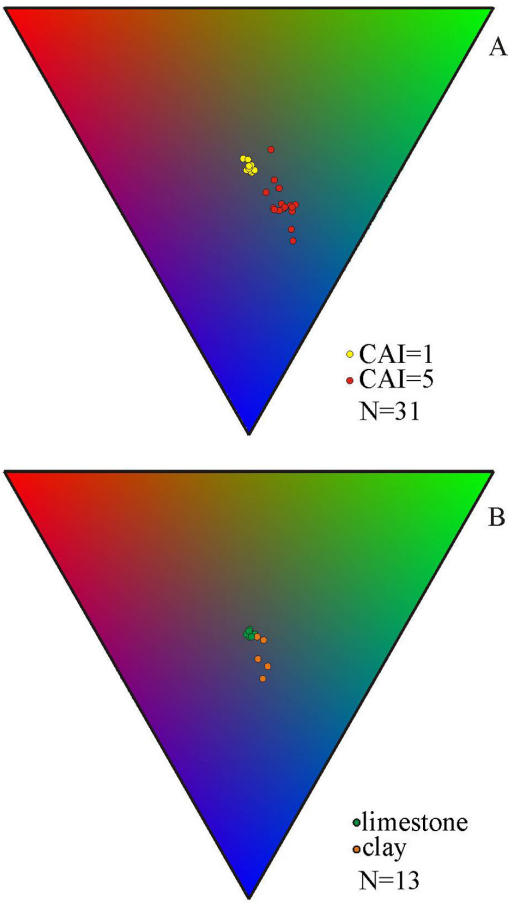

Fig. 5. Colour of cathodoluminescence of conodont elements on RGB diagram. A — CL of conodont elements with different CAI. B — CL of conodont elements from different host rocks (limestone and clay)

Рис. 5. Цвет катодолюминесценции конодонтовых элементов на RGB-диаграмме. A — CL элементов конодонтов с различным ИОК. B — CL элементов конодонтов из разных вмещающих пород (известняк и глина)

Organic molecules, which comprise up to 3% of conodont elements (Zhuravlev, 2023), may make some contribution to CL. Pure hydroxyapatite (HAP) has a grey or reddish CL, but pure collagen has a bluish-green CL (Barnett et al., 1975; Roman-Lopez et al., 2014). In RGB coordinates, the CL of all tissues of unaltered conodont elements is close to that of HAP and different from that of pure collagen (fig. 6). It is therefore reasonable to assume that organic matter contributes very little to the tone of conodont CL.

Ce, Eu, Sm, Mn induce bluish and blue-reddish CL (Richter et al., 2003, p. 154; Kempe & Götze, 2002). This colour of CL is observed in conodont elements derived from clay (figs. 2.9, b and 2.10, b). These conodont elements also show the presence of REE in their apatite. Mn^{2+} induces green to yellow CL (Richter et al., 2003, p. 154). CL is visible at very low Mn2+ concentrations ⩾1 ppm (Habermann et al., 1998), which is below the resolution of EDS (about 1000 ppm). The cumulative effect of Mn^{2+} and REE on the CL of conodont elements probably leads to orange to violet CL of conodont apatite. According to Götze (2012), blue CL emission can also be caused by lattice defects (electron defects on the oxygen of the phosphate group) (see also Habermann et al., 1997). Due to the complex nature of CL, it is difficult to distinguish the contribution of different factors.

The lack of gradient in CL from the outer to the inner part of a conodont element suggests that CL mainly reflects the near-primary composition of the conodont tissues and not only the secondary influx of contaminants from the host rock or ambient water. Conversely, the difference in CL between albid tissue (most resistant to chemical exchange with the environment) and other tissues suggests a significant contribution of external 'contaminants' to the CL of conodont elements.

In the case of corrosion of the conodont element surface in carbonate host rocks, the CL of the surface of the conodont element becomes reddish due to invasion

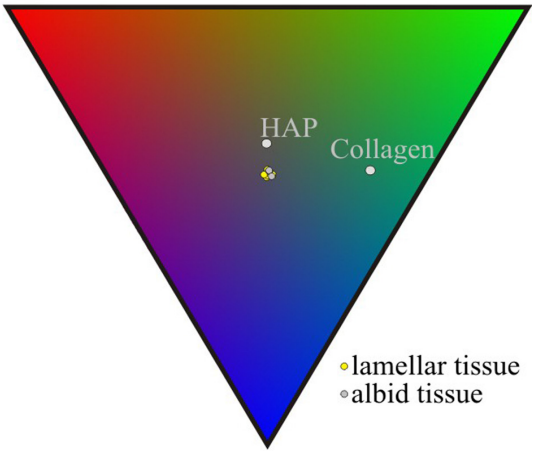

Fig. 6. Colour of cathodoluminescence of different tissues of conodont elements in comparison with pure HAP and collagen on RGB diagram

Рис. 6. Цвет катодолюминесценции различных тканей конодонтовых элементов в сравнении с чистым HAP и коллагеном на RGB-диаграмме

of the carbonate material (figs. 3.1, b and 3.2, b). In general, the CL of unaltered conodont elements is similar to that of unaltered shark teeth (blue), but differs significantly from that of fossil vertebrate teeth (orange-red).

Thus, CL data allow the detection of the results of secondary processes in conodont mineralised tissues, including enrichment by REE and/or Mn, corrosion and contamination by carbonate material. Therefore, CL of conodont elements can be used to screen significantly altered samples prior to chemical and isotopic investigations. For example, conodont elements showing evidence of carbonate incorporation with reddish CL cannot be used for carbon isotopic studies. This assumption is confirmed by the extremely high carbon isotope value of conodont elements showing reddish CL (sample 122-5/16, *Polygnathus parapetus Druce*, $\delta^{13}C_{con}$ = –22.5 ‰; mean $\delta^{13}C_{con}$ value for this species is –26.0 ‰).

Conclusions

CL allows tissue types to be distinguished on the basis of luminescence intensity and provides information on the histological composition of conodont elements. CL is also a promising tool for screening samples for ecogeochemical studies due to its sensitivity to post-mortem geochemical exchange between conodont elements and host rock. The violet and yellow shifts of CL colour can be used as a proxy for contamination of the conodont bioapatite during catagenesis. The results confirm that albid tissue is less affected by geochemical contamination and probably represents a near-primary composition of conodont elements.

Acknowledgements

The author thanks Viktor Radaev (CCU "Geonauka", Syktyvkar, Russia) for assistance with SEM, EDS, and SEM-CL, and A.A. Dornan for discussion on conodont ecogeochemistry. Also, author is grateful to DeepL Write for professional proofreading, and to reviewers for valuable suggestions improving the manuscript.

References

Balter V., Martin J. E., Tacail T., Suan G., Renaud S., Girard C. Calcium stable isotopes place Devonian conodonts as first level consumers // Geochemical Perspectives. 2019. 10. P. 36—39. DOI: 10.7185/geochemlet.1912

Barnett W. A., Wise M. L. H., & Jones E. C. Cathodoluminescence of biological molecules, macromolecules and cells // Journal of Microscopy. 1975. 105(3). P. 299—303. DOI: 10.1111/j.1365-2818.1975.tb04063.x

Götze J. Application of Cathodoluminescence Microscopy and Spectroscopy in Geosciences // Microscopy and Microanalysis. 2012. 18. P. 1270—1284. DOI: 10.1017/S1431927612001122

Griffin J. M., Montañez I. P., Glessner J. J. G., Chen J., Willmes M. Geologic variability of conodont strontium isotopic composition quantified by laser ablation multiple collection inductively coupled plasma mass spectrometry // Palaeogeography, Palaeoclimatology, Palaeoecology. 2021. 568. 110308. DOI: 10.1016/j.palaeo.2021.110308

Habermann D., Götze J., Neuser R. & Richter D. K. The phenomenon of intrinsic cathodoluminescence: Case studies of quartz, calcite and apatite // Zentralbl. Geol. Paläont. 1997. 1(10—12). P. 1275—1284.

Habermann D., Neuser R. D., & Richter D. K. Low limit of Mn^{2+}-activated cathodoluminescence of calcite: state of the art // Sedimentary Geology. 1998. 116(1—2). P. 13—24. DOI: 10.1016/s0037-0738(97)00118-8

Harris A. G. & Sweet W. C. Mechanical and chemical techniques for separating microfossils from rock. sediment and residue matrix. In: Feldmann R. M., Chapman R. E. & Hannibal J. T. (Eds), Paleotechniques // Paleontol. Soc. Spec. Publ. 1989. 4. P. 70—86.

Joachimski M. M., Buggisch W. Conodont apatite $\delta^{18}O$ signatures indicate climate cooling as a trigger of the Late Devonian mass extinction // Geology. 2002. 30(8). P. 711—714.

Kempe U. & Götze J. Cathodoluminescence (CL) behavior and crystal chemistry of apatite from rare-metal deposits // Mineral Magazine. 2002. 66. P. 135—156.

Kürschner W., Becker R. T., Buhl D., Veizer J. Strontium isotopes in conodonts: Devonian–Carboniferous transition, the northern Rhenish Slate Mountains, Germany // Ann. Soc. géol. Belg. 1992. 115 (2). P. 595—621.

Luz, B., Kolodny, Y., Kovach, J. Oxygen isotope variations in phosphate of biogenic apatites, III. Conodonts // Earth and Planetary Science Letters. 1984. 69. P. 255—262.

Richter D. K., Gotte T., Gotze J., & Neuser R. D. Progress in application of cathodoluminescence (CL) in sedimentary petrology // Mineralogy and Petrology. 2003. 79(3—4). P. 127—166. DOI: 10.1007/s00710-003-0237-4

Roman-Lopez J., Correcher V., Garcia-Guinea J., Rivera T., Lozano I. B. Thermal and electron stimulated luminescence of natural bones, commercial hydroxyapatite and collagen // Spectrochimica Acta Part A: Molecular and Biomolecular Spectroscopy. 2014. 120. P. 610—615, DOI: 10.1016/j.saa.2013.10.027

Schneider C. A., Rasband W. S., & Eliceiri K. W. NIH Image to ImageJ: 25 years of image analysis // Nature Methods. 2012. 9(7). P. 671—675. DOI: 10.1038/nmeth.2089

Ségalen L., de Rafelis M., Lee-Thorp J. A., Maurer A.-F., Renard M. Cathodoluminescence tools provide clues to depositional history in Miocene and Pliocene mammalian teeth // Palaeogeography, Palaeoclimatology, Palaeoecology. 2008. 266. P. 246—253.

Trotter J. A., Korsch M. J., Nicoll R. S., Whitford D. J. Sr isotopic variation in single conodont elements: implications for defining the Sr seawater curve. In: Sepagli E. (Ed), Seventh European Conodont Symposium. Studies on Conodonts // Bolletino Della Societa Paleontologica Italiana. 1999. P. 507—514

Trotter J. A. & Eggins S. M. Chemical systematics of conodont apatite determined by laser ablation ICPMS // Chemical Geology. 2006. 233. P. 196—216. DOI: 10.1016/j.chemgeo.2006.03.004

Ulian G., Moro D., Valdrè G. Hydroxylapatite and Related Minerals in Bone and Dental Tissues: Structural, Spectroscopic and Mechanical Properties from a Computational Perspective // Biomolecules. 2021. 11(5). 728. DOI: 10.3390/biom11050728

Wierzbowski H. Advances and Challenges in Palaeoenvironmental Studies Based on Oxygen Isotope Composition of Skeletal Carbonates and Phosphates // Geosciences. 2021. 11. 419. DOI: 10.3390/geosciences11100419

Wierzbowski H., Szaniawski H., & Błażejowski B. Structural, chemical and isotope evidence for secondary phosphate mineralization of grasping spines of Early Palaeozoic chaetognaths // Lethaia. 2021. 54. P. 245—259. DOI: 10.1111/let.12400

Zhuravlev A. V. Trophic position of some Late Devonian-Carboniferous (Mississippian) conodonts revealed on carbon organic matter isotope signatures: a case study of the East European basin // Geodiversitas. 2020. 42(24). P. 443—453. DOI: 10.5252/geodiversitas2020v42a24

Zhuravlev A. V. Carbon isotope study of conodont elements: applications and limitations // Marine Micropaleontology. 2023. 178. 102200 DOI: 10.1016/j.marmicro.2022.102200

Zhuravlev A. V. & Shevchuk S. S. Strontium distribution in Upper Devonian conodont elements: a palaeobiological proxy // Rivista Italiana di Paleontologia e Stratigrafia. 2017. 123(2). P. 203—210. DOI: 10.13130/2039-4942/8311

Zhuravlev A. V., Plotitsyn A. N. & Gruzdev D. A. Carbon Isotope Ratios in the Apatite-Protein Composites of Conodont Elements — Palaeobiological Proxy. In: Frank-Kamenetskaya O. V., Vlasov D. Y., Panova E. G., Lessovaia S. N. (eds), Processes and Phenomena on the Boundary between Biogenic and Abiogenic Nature. Springer, Cham: 2020. P. 749—764. DOI: 10.1007/978-3-030-21614-6_40

Поступила в редакцию / Received 07.04.2023